Model Parametrization and Adaptation Based on the Invariance of Support Vectors With Applications to Battery State-of-Health Monitoring

Caihao Weng, Jing Sun, *Fellow, IEEE*, and Huei Peng

***Abstract*—Support vector regression (SVR) algorithms have been applied to the identification of many nonlinear dynamic systems due to their excellent approximation and generalization capability. However, the standard SVR algorithm involves an iterative optimization process, which is often computationally expensive and inefficient. For applications such as the battery state-of-health (SOH) monitoring, where the identification algorithm needs to be applied repeatedly for multiple cells because of the variation in model dynamics (due to battery aging and cell-to-cell difference), the computational burden could pose difficulties for real-time or onboard implementation. In this paper, the battery $V-Q$ curve identification problem for SOH monitoring is studied. Based on experimental battery aging data, we develop a model parametrization and adaptation framework utilizing the simple structure of SVR representation with determined support vectors (SVs) so that the model parameters can be estimated in real time. Through mathematical analysis and simulations using a mechanistic battery aging model, it is shown that the SVs of the battery models stay invariant, even when the batteries age or vary. The invariance of the SVs is verified using experimental aging data. Consequently, the resulting model for the battery $V-Q$ curve can be directly incorporated into the battery management system (BMS) and adapted online for SOH monitoring. Moreover, the general characteristics of the data that could maintain the SVR invariance are identified. The proposed automated model parametrization process (via an optimization algorithm) can be extended to nonlinear dynamic systems with the given properties.**

***Index Terms*—Battery management systems (BMSs), lithium-ion batteries, model parametrization, state of health (SOH), support vector regression (SVR).**

NOMENCLATURE

x	Support vector (SV) model input.
y	SV model output.
μ	Constant term of SV model.
ε	Maximum tolerated estimation error.
w	Weighting parameter for constraint tightness.
β	Kernel coefficient of SV model.
α^+, α^-	Nonnegative decomposition of β.
ξ^+, ξ^-	Slack variables for constraint relaxation.
s^+, s^-	Slack variables for equality constraints.
$\mathbf{K}$	Kernel matrix.
$\mathbf{A}$, $\mathbf{b}$, $\mathbf{c}$, $\boldsymbol{\chi}$	Constraint matrix, constraint vector, objective vector, and decision variable of the reformulated standard linear programming.
$\mathbf{B}$	Optimal basis matrix.
Ω	Set of indexes for optimal basis.
sv	Identified SVs.
N	Number of data points used for regression.
N_{sv}	Number of identified SVs.
v	Battery terminal voltage.
q	Battery charged capacity.

Manuscript received May 19, 2014; revised August 21, 2014; accepted October 17, 2014. Date of publication October 22, 2014; date of current version September 15, 2015. This work was supported in part by the U.S.–China Clean Energy Research Center-Clean Vehicle Consortium (CERC-CVC) and in part by the U.S. Department of Energy under Award DE-PI0000012. The review of this paper was coordinated by Dr. M. Kazerani.

C. Weng is with the Department of Naval Architecture and Marine Engineering, University of Michigan, Ann Arbor, MI 48109-2102 USA (e-mail: chsweng@umich.edu).

J. Sun is with the Department of Naval Architecture and Marine Engineering, University of Michigan, Ann Arbor, MI 48109-2102 USA, and also with the Department of Electrical Engineering and Computer Science, University of Michigan, Ann Arbor, MI 48109-2102 USA (e-mail: jingsun@umich.edu).

H. Peng is with Department of Mechanical Engineering, University of Michigan, Ann Arbor, MI 48109 USA (e-mail: hpeng@umich.edu).

Color versions of one or more of the figures in this paper are available online at http://ieeexplore.ieee.org.

Digital Object Identifier 10.1109/TVT.2014.2364554

I. INTRODUCTION

THE RESEARCH and development of rechargeable energy storage systems has moved at an unprecedented pace in recent years, driven primarily by interests in improving system reliability, achieving higher system efficiency, and reducing environmental impact [1]–[3]. Among the various choices of energy storage technologies, lithium-ion systems stand out due to their superior portability and energy efficiency [4]–[6].

One major challenge for battery energy management is battery state-of-health (SOH) monitoring, particularly onboard detection of capacity fading during operations [7]–[11]. In our previous work, an incremental capacity analysis (ICA)-based battery capacity estimation method was proposed for onboard implementation [12]. The ICA technique differentiates the battery charged capacity Q with respect to the terminal voltage V, and transforms the plateaus of the voltage curve into clearly identifiable dQ/dV peaks on the incremental capacity (IC) curve [13], [14]. The efficacy of ICA has been shown with various lithium-ion batteries ($LiFePO_4$, LiNMC, LNCAO, $LiMn_2O_4$, etc.) [13], [15]–[18]. One alternative way of extracting the battery aging signature and analyzing battery SOH from the voltage curve is the differential voltage analysis (DVA) [19]. In contrast to the ICA, the DVA is based on the dV/dQ curve. The accuracy of DVA-based capacity fading prediction has been shown in [20] and [21]. The major difficulty in performing ICA and DVA is the sensitivity to noise in

battery voltage measurement, particularly for $LiFePO_4$ batteries [16]–[18]. Since all the peaks on an IC curve lie within the flat region of the $V-Q$ curve, computing the derivatives directly from the data could lead to inaccurate and undesirable results, even after careful data filtering. This issue was successfully addressed by using the SV regression (SVR) algorithm, as discussed in [12].

The SVR method is the application of the SV algorithm, which was initially developed by Drucker *et al.* at the AT&T Bell Laboratories, for data regression [22]. It has been an active area of research and played a significant role in solving problems such as data classification and function estimation over the last two decades [23]–[26]. The method relies on the use of the kernel trick, which maps data points to a higher dimensional feature space through an inner product to make them linearly separable, so that a nonlinear separating surface can be represented with a linear model in the feature space [23], [27]. Consequently, the nonlinear data can be estimated and classified using linear methods, as long as the problem is formulated in terms of kernel evaluations [28], [29].

Different from the SV algorithm for data classification (e.g., output $y \in \{\pm 1\}$ in a two-classes case), the SVR problem is concerned with estimating real-valued functions (i.e., output $y \in \mathbb{R}$) [27]. By incorporating the ε-insensitive loss function, a regression problem is constructed such that a function $f(x)$ that has at most ε deviation from the target values y can be found [25], [27], [30]. In this case, estimation errors less than ε are treated as zero, and only the losses greater than ε is concerned in the objective function. It has been shown that the use of ε-insensitive loss function yields sparse and, thus generalizable, solutions [31].

Despite the simple structure, the standard SVR algorithm involves solving an optimization problem whose dimension depends on the size of the training data set and, therefore, requires nontrivial computational efforts to determine the kernel parameters. Since the resulting high-dimensional optimization process is often computationally expensive, the potential applications are limited, particularly for onboard and real-time estimation problems.

Moreover, unlike most SVR problems where the optimization is only performed once, for applications such as the SOH monitoring of a multiple-cell battery system, the algorithm needs to be applied to every cell individually and repeatedly due to aging and cell-to-cell variations. The need for repeated optimization can dramatically increase the computational burden and make the real-time implementation on a resource-limited platform difficult or impossible.

Motivated by our initial success in applying the SVR for battery SOH monitoring (reported in [12]) as well as the associated computational challenges identified in the process, this paper aims to develop an onboard implementable model parametrization and adaptation framework. More specifically, we will exploit the simple structure of SVR representation, and study under what conditions the parametric model of battery $V-Q$ curves identified from one reference cell can be applied to different cells at different aging stages. If the SVs remain invariant from the SVR model of one cell to another, or from one aging state to another, then only the coefficients of the SVR model need to be updated for model identification. Furthermore, given the special sampling scheme, we can eliminate the iterative optimization procedure altogether. This framework could greatly reduce the computational load as the resulting model parameters can be estimated in real time. Moreover, the parametric structure could help us to better understand the physical properties of the underlying problems and take advantage of the knowledge we have about the systems [32].

This paper reports the findings of exploiting the parametric SVR model for real-time battery system characterization, and proposes a framework for online battery SOH monitoring. The study is based on test data collected from eight A123 APR18650 cells, which use $LiFePO_4$ as the positive electrode material and graphite as the negative electrode. The data were collected over a period of 18 months [33]. The test data used for this study were acquired through a battery test bench, which includes an Arbin BT2000 tester, a thermal chamber for environment control, a computer for user–machine interface and data storage, a switchboard for cable connection, and battery cells [33]. The data acquisition system has a logging frequency of 10 Hz, and the measurement precision of both current and voltage is 0.02% (i.e., 1 mV for voltage measurement) [34].

The remainder of this paper is organized as follows. Section II formulates the linear programming SVR (LP-SVR) problem for the identification of $V-Q$ curve. Section III extends the general LP problem into a parametric LP problem with sensitivity study. Section IV shows the data variation when battery ages through simulation and actual test data. Section V solves the proposed parametric LP problem using Monte Carlo simulations and establishes the parametric model based on the invariance of the SVs. The conclusions are given in Section VI.

II. Battery $V-Q$ Curve and Support Vector Regression Model

A. Battery $V-Q$ Curve Identification for Incremental Capacity Analysis

ICA has the advantage of detecting a gradual change in cell behavior during a life-cycle test, with greater sensitivity than those based on conventional charge/discharge curves, and yielding key information on the cell behavior associated with its electrochemical properties [15], [35]. As shown in Fig. 1, which shows the test data at different aging stages for a $LiFePO_4$ battery, the IC curve [see Fig. 1(b)] has more identifiable aging signs than the $V-Q$ curve p [see Fig. 1(a)]. It is useful particularly for battery SOH monitoring as the extracted peak values and their change pattern on the IC curves are closely related to the battery capacity fading and can be used for characterizing the aging mechanism. However, because of measurement noise, performing the ICA directly from the measured $V-Q$ curve has proven to be not a viable option [12], [16], [18], [36], particularly for onboard battery management systemss (BMSs), where the measurement precision is limited; development of appropriate data processing functions is required so that ICA can

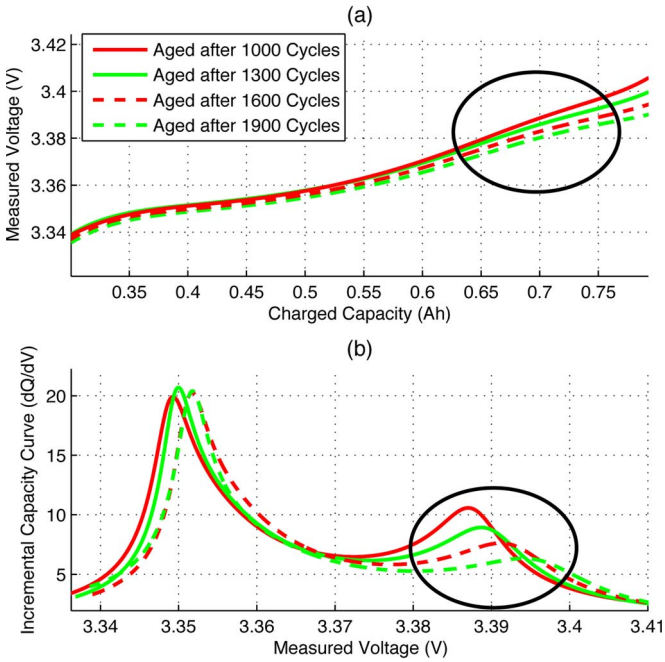

Fig. 1. Aging signature extracted using ICA.

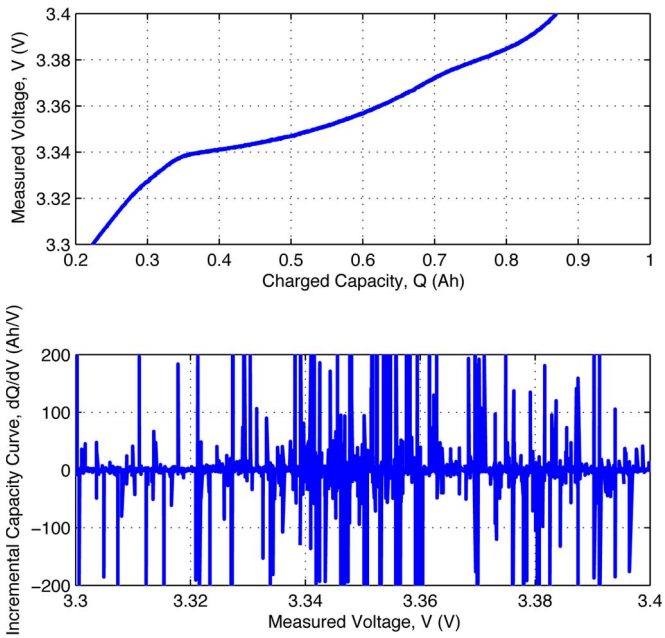

Fig. 2. Sensitivity of the numerically derived dQ/dV curve to measurement noise.

be applied. Fig. 2 shows how sensitive numerical differentiation is to the measurement noise.

In our previous work, several numerical procedures are developed and evaluated for extracting the IC curves from battery $V-Q$ data. While the ICA results are sensitive to the selection of the curve fitting method, the SVR approach with the Gaussian radial basis function (rbf) kernel is shown to be the most robust and effective method. Using SVR to represent the $V-Q$ relation and then using an analytic derivative to obtain the IC curve provide the most consistent identification results with moderate computational load [12].

B. Support Vector Regression Model

As discussed earlier, the SVR was chosen for the battery $V-Q$ curve identification because of its demonstrated potential in the realm of nonlinear system identification [37]–[39]. Let $x = q$, $y = v$ be the input and output of the SVR model, where q represents the battery charged capacity, and$v$ is the measured voltage. The SVR model for the $V-Q$ curve can thereby be represented as

$$y = \sum_{i=1}^{N} \beta_i \mathcal{K}(x_i, x) + \mu \tag{1}$$

where N is the number of data points in the data set, β_i and μ are the model parameters, whose values are determined based on the data set, and $\mathcal{K}(\cdot,\cdot)$ is the selected kernel. In this paper, the rbf kernel is used and is expressed as

$$\mathcal{K}(x, x') = \exp\left(\frac{-\|x - x'\|^2}{2\sigma^2}\right) \tag{2}$$

where σ is the adjustable parameter for the kernel function.

The parameters used in model (1) are identified by solving a convex quadratic programming (QP) problem. Through the QP-SVR and appropriate selected kernel, the flatness property is enforced in both the feature space and input space [25], [37]. Conventional QP-SVR has been successfully applied in identifying nonlinear dynamic systems [37], [39], [40]. However, the implementation of QP-SVR may not guarantee sufficient model sparsity. LP-SVR that employs an ℓ_1 norm as a regularizer was then proposed to improve the model sparsity and computational efficiency [38], [41]–[43]. In our previous work, LP was used as the optimization engine to derive the SVR model [12].

The SVR using ℓ_1 regularizer formulates the optimization problem as follows:

$$\min_{\boldsymbol{\beta},\mu,\boldsymbol{\xi}^+,\boldsymbol{\xi}^-} \|\boldsymbol{\beta}\|_1 + w\sum_{n=1}^{N}\left(\xi_n^+ + \xi_n^-\right)$$
$$\text{subject to } \begin{cases} \sum_{i=1}^{N}\beta_i\mathcal{K}(x_i, x_n) + \mu - y_n \le \varepsilon + \xi_n^+ \\ y_n - \sum_{i=1}^{N}\beta_i\mathcal{K}(x_i, x_n) - \mu \le \varepsilon + \xi_n^- \\ \boldsymbol{\xi}^+, \boldsymbol{\xi}^- \ge 0 \end{cases} \tag{3}$$

where ξ_n^+ and ξ_n^- are the slack variables introduced to cope with the infeasible constraints, w is the weighting factor, ε is the precision parameter, $\|\cdot\|_1$ denotes the ℓ_1 norm in the coefficient space, and $\boldsymbol{\beta}$ is defined as $\boldsymbol{\beta} = (\beta_1, \ldots, \beta_n)^T$. The optimal result usually gives zero value for most of the β_i, and the x_i corresponding to nonzero β_i are called SVs [25].

To establish the problem as an LP optimization, the coefficients β_i need to be decomposed (using the property of linear piecewise convex function minimization) as [44]

$$\beta_i = \alpha_i^+ - \alpha_i^- \quad |\beta_i| = \alpha_i^+ + \alpha_i^- \tag{4}$$

where α_i^+ and α_i^- are nonnegative and satisfy $\alpha_i^+ \cdot \alpha_i^- = 0$.

C. Formulation of Linear Programming Support Vector Regression

Following the derivation reported in [38], the SVR problem using ℓ_1 regularizer can be reformulated as an LP problem, i.e.,

$$\min \mathbf{c}^T \begin{pmatrix} \boldsymbol{\alpha}^+ \\ \boldsymbol{\alpha}^- \\ \boldsymbol{\xi}^+ \\ \boldsymbol{\xi}^- \\ \mu \end{pmatrix}$$

$$\text{subject to} \begin{cases} \begin{pmatrix} \mathbf{K} & -\mathbf{K} & -\mathbf{I} & 0 & 1 \\ -\mathbf{K} & \mathbf{K} & 0 & -\mathbf{I} & -1 \end{pmatrix} \begin{pmatrix} \boldsymbol{\alpha}^+ \\ \boldsymbol{\alpha}^- \\ \boldsymbol{\xi}^+ \\ \boldsymbol{\xi}^- \\ \mu \end{pmatrix} \\ \qquad \leq \begin{pmatrix} \varepsilon + \mathbf{y} \\ \varepsilon - \mathbf{y} \end{pmatrix} \\ \boldsymbol{\alpha}^+, \boldsymbol{\alpha}^-, \boldsymbol{\xi}^+, \boldsymbol{\xi}^- \geq 0 \end{cases} \tag{5}$$

where

$$\begin{aligned} \mathbf{c} &= \left(\underbrace{1, \ldots, 1}_{2N}, \underbrace{w, \ldots, w}_{2N}, 0 \right)^T \\ \mathbf{y} &= (y_1, \ldots, y_N)^T \\ \boldsymbol{\alpha}^+ &= \left(\alpha_1^+, \ldots, \alpha_N^+\right)^T \\ \boldsymbol{\alpha}^- &= \left(\alpha_1^-, \ldots, \alpha_N^-\right)^T \\ \boldsymbol{\xi}^+ &= \left(\xi_1^+, \ldots, \xi_N^+\right)^T \\ \boldsymbol{\xi}^- &= \left(\xi_1^-, \ldots, \xi_N^-\right)^T \end{aligned} \tag{6}$$

and $\mathbf{I}$ is an $N \times N$ identity matrix. $\mathbf{K}$ is the kernel matrix with entries defined as $K_{ij} = \mathcal{K}(x_i, x_j)$

$$\mathbf{K} = \begin{pmatrix} \mathcal{K}(x_1, x_1) & \mathcal{K}(x_1, x_2) & \cdots & \mathcal{K}(x_1, x_N) \\ \mathcal{K}(x_2, x_1) & \mathcal{K}(x_2, x_2) & \cdots & \mathcal{K}(x_2, x_N) \\ \vdots & \vdots & \ddots & \vdots \\ \mathcal{K}(x_N, x_1) & \mathcal{K}(x_N, x_2) & \cdots & \mathcal{K}(x_N, x_N) \end{pmatrix}. \tag{7}$$

The LP problem (5) is bounded and feasible by default and can always be solved using a standard algorithm such as the simplex method or the interior point method.

Fig. 3 shows how the LP-SVR algorithm is implemented for the identification of the battery $V-Q$ curve. First, the parameters in model (1) are determined, and the SVR model of the $V-Q$ curve, i.e.,

$$f(x_n) = \sum_{i=1}^{N_{\text{sv}}} \beta_i \mathcal{K}(\text{sv}_i, x_n) + \mu \tag{8}$$

is obtained, where sv_i $(i = 1, \ldots, N_{\text{sv}})$ are the SVs identified by the LP-SVR algorithm, and N_{sv} is the total number of SVs $(N_{\text{sv}} \ll N)$.

Then, the IC curve can be computed from the fitted $V-Q$ curve as follows:

$$\frac{dQ}{dV} = \frac{1}{f'(x_n)} = \frac{1}{\sum_{i=1}^{N_{\text{sv}}} \beta_i \mathcal{K}'(\text{sv}_i, x_n)}. \tag{9}$$

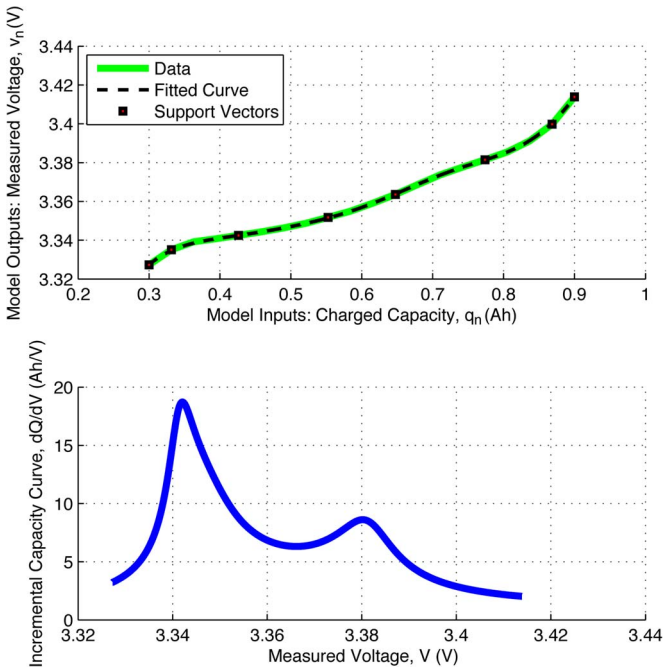

Fig. 3. Implementation of LP-SVR for battery $V-Q$ and IC curve identification.

Using the ICA technique, we can then extract battery aging information through the changes observed from the IC peaks. Please note that the correlation between battery capacity and IC peaks could be influenced by environmental temperature. Therefore, our SOH monitoring framework is designed based on battery charging data collected under constant temperature. We think it is a valid assumption since active thermal management systems are implemented on most commercial electric vehicles. On the other hand, since the ICA is mainly based on the lithium intercalation process, it might not be directly applicable to battery chemistries such as Pb–Acid and Ni–MH. Nonetheless, because voltage data of any battery cells are associated with their fading and degradation, it is possible that one could extract an aging signature (perhaps different from lithium-ion batteries) using the dQ/dV analysis from those chemistries as well.

Although LP-SVR works well for retrieving the IC curve from battery voltage measurement, it has to be applied repeatedly to different cells at different ages. For applications such as electric vehicles, which usually contain hundreds or thousands of battery cells, the extensive computational effort required for solving the LP problems could not be satisfied on-board or in real time.

If the simple structure produced by the LP-SVR, (8), can be generalized as a parametric model with kernel functions as the basis and the SVs invariant, for all cells under all conditions, conventional parameter estimation methods such as the least squares can be directly used, and the computational efficiency would be greatly improved. In this case, the LP-SVR algorithm is only used for the initial model identification and parametrization, whereas the parameter adaptation to fit individual cell data and aging status could be achieved through linear parameter identification that does not require iterative optimization.

III. Conditions for Support Vectors Invariance and Parametric Linear Programming

To investigate the possibility of using the SVR model as a parametric model with invariant SVs, an LP sensitivity study is performed to understand the variations of the SVs with respect to the data variation. For the convenience of performing LP sensitivity study, we can transform problem (5) into a standard LP formulation, i.e.,

$$\min_{\boldsymbol{\chi}} \quad \mathbf{c}^T\boldsymbol{\chi} \qquad \text{subject to} \quad \begin{cases} \mathbf{A}\boldsymbol{\chi} = \mathbf{b} \\ \boldsymbol{\chi} \geq 0 \end{cases} \tag{10}$$

where

$$\begin{aligned} \mathbf{c} &= \left(\underbrace{1,\ldots,1}_{2N},\underbrace{w,\ldots,w}_{2N},\underbrace{0,\ldots,0}_{2N+2}\right)^T \\ \boldsymbol{\chi} &= \left(\boldsymbol{\alpha}^+;\boldsymbol{\alpha}^-;\boldsymbol{\xi}^+;\boldsymbol{\xi}^-;\mu^+;\mu^-;\mathbf{s}^+;\mathbf{s}^-\right) \\ \mathbf{A} &= \begin{pmatrix} \mathbf{K} & -\mathbf{K} & -\mathbf{I} & 0 & 1 & -1 & \mathbf{I} & 0 \\ -\mathbf{K} & \mathbf{K} & 0 & -\mathbf{I} & -1 & 1 & 0 & \mathbf{I} \end{pmatrix} \\ \mathbf{b} &= \begin{pmatrix} \varepsilon + \mathbf{y} \\ \varepsilon - \mathbf{y} \end{pmatrix} \\ \mu &= \mu^+ + \mu^- \end{aligned} \tag{11}$$

μ^+ and μ^- are added to ensure nonnegativity on the decision variable, and $\mathbf{s}^+$ and $\mathbf{s}^-$ are added to convert the inequality constraints into equality. This new formulation is equivalent to the original problem (5) [44].

A. Formulation of Parametric Linear Programming

Let us assume that we have found an optimal basis matrix $\mathbf{B}$ for the standard LP problem, where

$$\mathbf{B} = \begin{pmatrix} \mathbf{A}_{\Omega(1)} & \mathbf{A}_{\Omega(2)} & \cdots & \mathbf{A}_{\Omega(m)} \end{pmatrix} \tag{12}$$

and $\mathbf{A}_{\Omega(1)},\ldots,\mathbf{A}_{\Omega(m)}$ are linear independent columns chosen as the optimal basis from the constraint matrix $\mathbf{A}$. Then, $\mathbf{B}$ must satisfy the following conditions [44]:

$$\begin{aligned} &\mathbf{B}^{-1}\mathbf{b} \geq 0 \\ &\mathbf{c} - \mathbf{c}_\mathbf{B}\mathbf{B}^{-1}\mathbf{A} \geq 0 \end{aligned} \tag{13}$$

where $\mathbf{c}_\mathbf{B}$ consists of the entries in the objective vector $\mathbf{c}$ corresponding to the optimal basis matrix $\mathbf{B}$, i.e.,

$$\mathbf{c}_\mathbf{B} = \begin{pmatrix} \mathbf{c}_{\Omega(1)} & \mathbf{c}_{\Omega(2)} & \cdots & \mathbf{c}_{\Omega(m)} \end{pmatrix}^T. \tag{14}$$

Now, consider the different LP problem (10) for a different data set that is obtained either for a different cell or for the same cell at a different aging stage. In our study, the battery charging data are always sampled between the same range of charged capacity with the same rate (i.e., the variable $\mathbf{x}$ in problem (3) does not change from cell to cell and time to time). Although this might appear to be a limitation of the technique for on-board implementation, those data samples should be available for SOH monitoring periodically during normal operations as the range of the charged capacity data that we are using is within the typical operating range of electric vehicles. Because of the sampling scheme, the matrix $\mathbf{K}$ and the constraint matrix $\mathbf{A}$ do not vary as the data set changes. In addition, the objective vector $\mathbf{c}$ is always kept constant. The only term that is changed is $\mathbf{b}$ in the constraint. Therefore, the condition $\mathbf{c} - \mathbf{c}_\mathbf{B}\mathbf{B}^{-1}\mathbf{A} \geq 0$ is always satisfied even when data variation occurs. The optimal condition for the original optimal basis matrix $\mathbf{B}$ to be satisfied by the new data set can then be reduced to

$$\mathbf{B}^{-1}\mathbf{b} \geq 0. \tag{15}$$

Since the optimal basis matrix $\mathbf{B}$ decides the values of the SVs, it can be concluded that the SVs for the battery $V-Q$ curve model would not change if, given $\mathbf{B}$, (15) is satisfied for the new data set. If (15) is satisfied for all data sets collected for different cells and at different aging stages, we call the SVs invariant, and the same SVs and basis functions can be used to represent different $V-Q$ characteristics for different cells and at different time.

Moreover, $\mathbf{b}$ only depends on the variable $\mathbf{y}$, which is the voltage measurement from the battery charging data. Hence, the sensitivity analysis only needs be performed with respect to $\mathbf{y}$ in this paper, and problem (10) can be rewritten as

$$\min \quad \mathbf{c}^T\boldsymbol{\chi} \qquad \text{subject to} \quad \begin{cases} \mathbf{A}\boldsymbol{\chi} = \mathbf{b}(\mathbf{y}) \\ \boldsymbol{\chi} \geq 0. \end{cases} \tag{16}$$

The formulation shown in problem (16) is typically referred to as parametric LP [45]. In conventional parametric LP problems, the dependence of $\mathbf{b}$ on the varying parameters is usually linear. One can find the correspondence between all the optimal basis and the varying parameters by solving systems of linear equalities. However, in our battery $V-Q$ identification problem, the data variation is nonlinear, and a proper parametrization needs to be found for characterizing the variation.

B. Special Scenario: Constant Shift in the Battery Data

Before proceeding to more complex cases, let us first consider the special scenario: constant shift in the battery data. Let $\mathbf{y}_1$ be the reference data set, and $\mathbf{y}_2$ be the data set with a constant shift (i.e., $\mathbf{y}_2 = \mathbf{y}_1 + \rho$). We have the following proposition.

Proposition 3.1: A constant shift in the data does not change the SVs.

Proof: Assume that the optimal solution of (16) corresponding to the data $\mathbf{y}_1$ is $\boldsymbol{\chi}_*$, where

$$\boldsymbol{\chi}_* = \left(\boldsymbol{\alpha}_*^+;\boldsymbol{\alpha}_*^-;\boldsymbol{\xi}_*^+;\boldsymbol{\xi}_*^-;\mu_*^+;\mu_*^-;\mathbf{s}_*^+;\mathbf{s}_*^-\right). \tag{17}$$

Note that the column vectors in $\mathbf{B}$ that correspond to μ^+ or μ^- are not related to the invariance of SVs, and they can be treated independently from the rest of the basis vectors. For that reason,

let $\hat{\boldsymbol{\chi}}_*$ and $\hat{\mathbf{A}}$ be the submatrices of $\boldsymbol{\chi}_*$ and $\mathbf{A}$, excluding the columns associated with μ^+ or μ^-, respectively. That is

$$\hat{\mathbf{A}} = \begin{pmatrix} \mathbf{K} & -\mathbf{K} & -\mathbf{I} & 0 & \mathbf{I} & 0 \\ -\mathbf{K} & \mathbf{K} & 0 & -\mathbf{I} & 0 & \mathbf{I} \end{pmatrix}$$
$$\hat{\boldsymbol{\chi}}_* = \left(\boldsymbol{\alpha}_*^+; \boldsymbol{\alpha}_*^-; \boldsymbol{\xi}_*^+; \boldsymbol{\xi}_*^-; \mathbf{s}_*^+; \mathbf{s}_*^-\right). \tag{18}$$

We then have

$$\hat{\mathbf{A}}\hat{\boldsymbol{\chi}}_* + \begin{pmatrix} 1 & -1 \\ -1 & 1 \end{pmatrix} \begin{pmatrix} \mu_*^+ \\ \mu_*^- \end{pmatrix} = \mathbf{A}\boldsymbol{\chi}_* = \mathbf{b}(\mathbf{y_1}) = \begin{pmatrix} \varepsilon + \mathbf{y}_1 \\ \varepsilon - \mathbf{y}_1 \end{pmatrix}. \tag{19}$$

On the other hand, let

$$\begin{pmatrix} 1 & -1 \\ -1 & 1 \end{pmatrix} \begin{pmatrix} \mu^+ \\ \mu^- \end{pmatrix} = \begin{pmatrix} 1 & -1 \\ -1 & 1 \end{pmatrix} \begin{pmatrix} \mu_*^+ \\ \mu_*^- \end{pmatrix} + \begin{pmatrix} 1 \\ -1 \end{pmatrix} \rho. \tag{20}$$

By substituting (20) into (19), the following equation is obtained:

$$\begin{aligned} &\hat{\mathbf{A}}\hat{\boldsymbol{\chi}}_* + \begin{pmatrix} 1 & -1 \\ -1 & 1 \end{pmatrix} \begin{pmatrix} \mu^+ \\ \mu^- \end{pmatrix} \\ &= \hat{\mathbf{A}}\hat{\boldsymbol{\chi}}_* + \begin{pmatrix} 1 & -1 \\ -1 & 1 \end{pmatrix} \begin{pmatrix} \mu_*^+ \\ \mu_*^- \end{pmatrix} + \begin{pmatrix} 1 \\ -1 \end{pmatrix} \rho \\ &= \begin{pmatrix} \varepsilon + \mathbf{y}_1 \\ \varepsilon - \mathbf{y}_1 \end{pmatrix} + \begin{pmatrix} 1 \\ -1 \end{pmatrix} \rho = \begin{pmatrix} \varepsilon + \mathbf{y}_1 + \boldsymbol{\rho} \\ \varepsilon - \mathbf{y}_1 - \boldsymbol{\rho} \end{pmatrix} \\ &= \begin{pmatrix} \varepsilon + \mathbf{y}_2 \\ \varepsilon - \mathbf{y}_2 \end{pmatrix} = \mathbf{b}(\mathbf{y}_2) \end{aligned} \tag{21}$$

where one should see that the change in ρ would be compensated by adjusting either μ^+ or μ^-, without affecting the value of $\hat{\boldsymbol{\chi}}_*$. The LP problems with $\mathbf{y}_1$ and that with $\mathbf{y}_2$ share the same $\hat{\boldsymbol{\chi}}_*$ as part of their optimal solutions. Therefore, the variation in the constant term ρ does not change the SVs.

IV. Voltage Data Variation

A. Characterization of Battery Data Variation Using Mechanistic Battery Aging Model Simulation

The variation in battery voltage measurement during aging could be simulated using the mechanistic battery aging model developed in [46]. The battery model considers the aging mechanism of both the positive and negative electrodes and could reflect the qualitative relationship between the equilibrium potentials and battery aging status. Fig. 4 shows the equilibrium potentials of $LiFePO_4$ batteries. The analytic models for the equilibrium potentials can be found in literature [47], [48]. The overall equilibrium potential of the battery cell is the difference between the positive electrode and the negative electrode: $V_{\text{total}} = V_{\text{PE}} - V_{\text{NE}}$ (see Fig. 5).

As discussed in [17], the capacity fading in $LiFePO_4$ cells is mainly caused by the loss of cycable lithium at the early stages of aging. The loss of cycable lithium could be simulated by shifting the relative location of the two potential curves [46]. The simulation results are shown in Fig. 6, where the voltage output of the model of the aged cells V_{aged} is plotted versus the output of the reference cell V_{ref}, which represents a new battery.

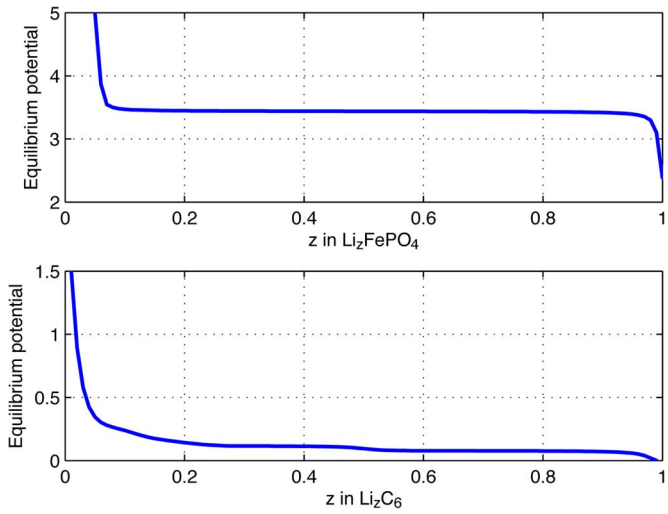

Fig. 4. Equilibrium potentials of $LiFePO_4$ batteries.

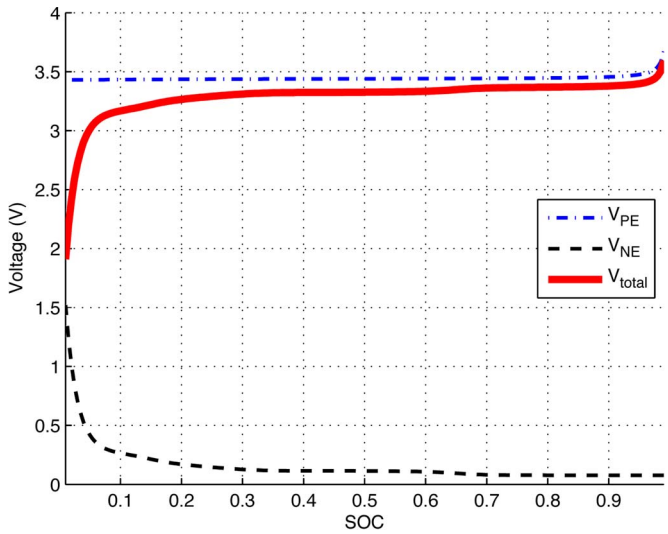

Fig. 5. Open-circuit voltage of $LiFePO_4$ batteries simulated using the mechanistic battery aging model from [46].

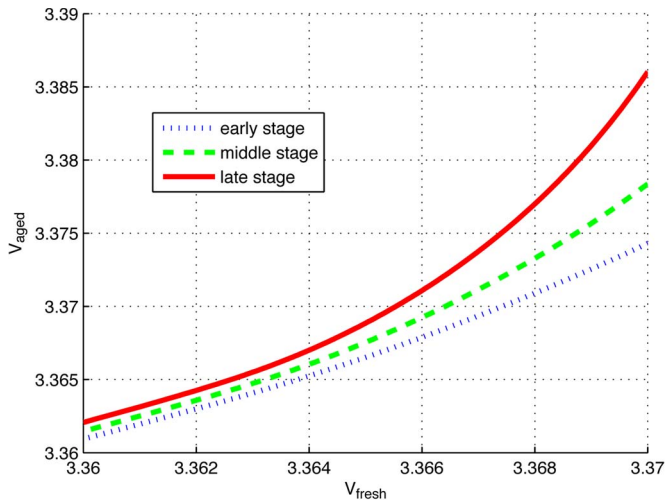

Fig. 6. Simulated voltage variations of $LiFePO_4$ batteries at different aging stages.

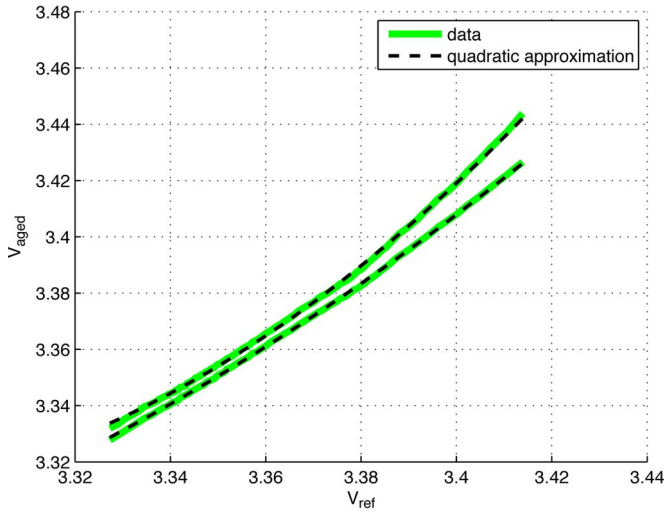

Fig. 7. Voltage variation of $LiFePO_4$ batteries observed in the test data at $T = 35\,^{\circ}\mathrm{C}$.

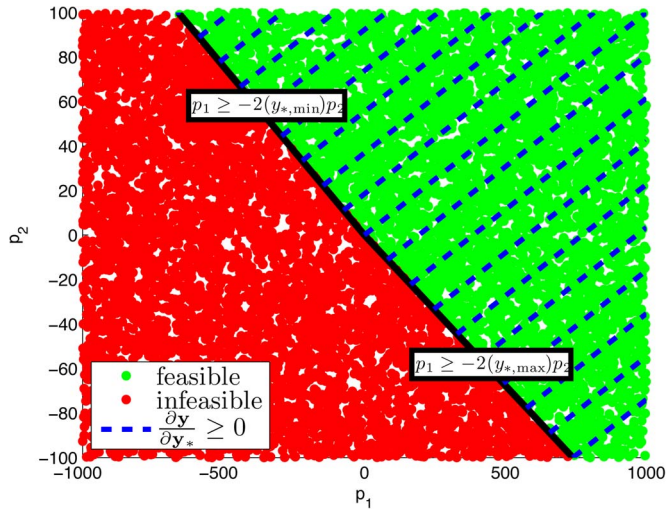

Fig. 8. Monte Carlo simulations for determining feasible region of (p_1, p_2) corresponding to the optimal basis $\mathbf{B}$.

It is observed that the relation between V_{aged} and V_{ref} could be approximated by a quadratic function, i.e.,

$$\mathbf{y} = p_2 \mathbf{y}_*^2 + p_1 \mathbf{y}_* + p_0 \tag{22}$$

where p_0, p_1, and p_2 are the parameters of the quadratic function.

B. Data Verification

The quadratic approximation (22) found using the mechanistic battery aging model that relates the voltage response of the aged cell to that of a fresh new cell can be verified with the actual test data. As aforementioned, the data used in this paper are collected from eight A123 APR18650 cells over a period of 18 months. Fig. 7 shows two sets of data variation at different aging stages. The curves can be fitted with quadratic functions with good accuracy.

Hence, the quadratic function is indeed a good approximation and can be used for characterizing the voltage variation.

V. Invariance of the Support Vectors and Linear Parametric Model

A. Results from Monte Carlo Simulations

Since the characteristics of voltage variation are identified, we can then investigate under what conditions the optimal basis computed from the reference data stays invariant when the parameters of the quadratic function vary as the cell ages. In particular, we are interested in finding the following feasible region for SV invariance. Assuming that the problem

$$\begin{aligned} \min \quad & \mathbf{c}^T \boldsymbol{\chi} \\ \text{subject to} \quad & \begin{cases} \mathbf{A}\boldsymbol{\chi} = \mathbf{b}(\mathrm{y}_*) \\ \boldsymbol{\chi} \geq 0 \end{cases} \end{aligned} \tag{23}$$

has the optimal basis $\mathbf{B}$, then for any pair of p_1 and p_2, if the corresponding $\mathbf{b}(\mathbf{y})$ satisfies $\mathbf{B}^{-1}\mathbf{b}(\mathbf{y}) \geq 0$, the pair (p_1, p_2) is considered feasible. Otherwise, the pair is infeasible.

As discussed earlier (see Prop. 3.1), the variation in the constant term p_0 does not affect the invariance of the SVs, and it can be ignored in solving the parametric LP problems.

Different from the general approaches for solving the conventional parametric LP problems, the dependence of $\mathbf{b}$ on the varying parameters p_1 and p_2 is nonlinear. Instead of solving systems of linear equalities, the determination of feasibility for each parameter pair (p_1, p_2) is done through Monte Carlo simulations. The results are shown in Fig. 8, where the green region highlights the feasible region.

On the other hand, we can find the region, where $\mathbf{y}$ and $\mathbf{y}_*$ have a monotonic increasing relation, by computing

$$\frac{\partial \mathbf{y}}{\partial \mathbf{y}_*} = 2p_2 \mathbf{y}_* + p_1 \geq 0 \tag{24}$$

and therefore, the region (marker by blue dashed lines in Fig. 8) is defined by the following two boundary functions:

$$\begin{aligned} p_1 &\geq -(2y_{*,\min})p_2 \\ p_1 &\geq -(2y_{*,\max})p_2. \end{aligned} \tag{25}$$

From the simulation results shown in Fig. 8, one can see that the feasible region computed by the Monte Carlo simulations coincides with the region where $\mathbf{y}$ is monotonic increasing. The results imply that the SVs for the battery $V-Q$ curve model would stay invariant as long as the variation in the voltage data satisfies a quadratic and monotonic increasing relationship. As shown in Figs. 5 and 6, the monotonic quadratic relationship is consistent with our simulation results and observations from the battery data.

B. Model Parametrization

According to the analysis performed earlier, the SVs should not change even when battery ages or varies for our applications. Fig. 9 show the LP-SVR results for the data of one cell at different ages. The invariance of the SVs can be clearly observed from the plot. Therefore, the structure obtained by

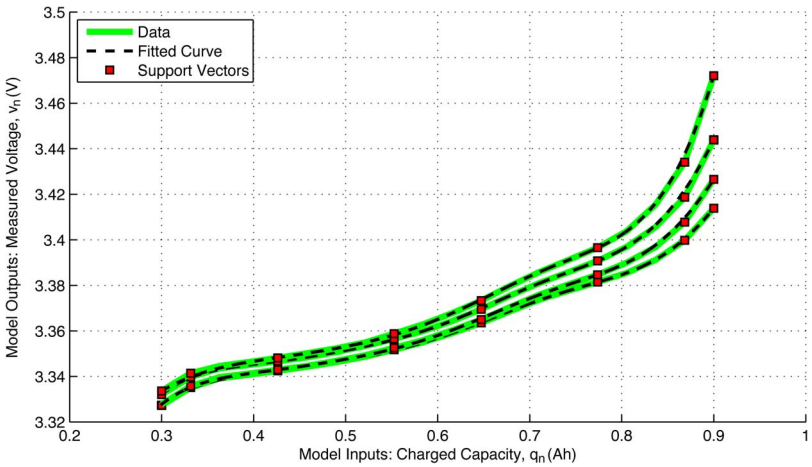

Fig. 9. Invariance of SVs from LP-SVR results.

the initial LP-SVR results can be used as a parametric model for the identification of battery $V-Q$ curves. The model is parametrized as follows:

$$v = \sum_{i=1}^{N_{\rm sv}} \beta_i \mathcal{K}(\mathrm{sv}_i, q) + \mu. \tag{26}$$

For onboard implementation, the estimation problem of the model parameters $\boldsymbol{\beta}$ and μ can be formulated as follows:

$$v_j = \boldsymbol{\theta}^T \boldsymbol{\phi}_j \tag{27}$$

where

$$\begin{aligned} \boldsymbol{\theta} &= [\boldsymbol{\beta}^T, \mu]^T \\ \boldsymbol{\phi}_j &= [\mathcal{K}(\mathrm{sv}_1, q_j), \ldots, \mathcal{K}(\mathrm{sv}_{N_{\rm sv}}, q_j), 1]^T \\ \boldsymbol{\beta} &= [\beta_1, \ldots, \beta_{N_{\rm sv}}]^T \end{aligned} \tag{28}$$

and the parameters could be solved by the standard least squares method (LSM)

$$\boldsymbol{\theta} = \left(\boldsymbol{\Phi}^T \boldsymbol{\Phi}\right)^{-1} \boldsymbol{\Phi}^T \mathbf{V} \tag{29}$$

where

$$\begin{aligned} \mathbf{V} &= [v_1, \ldots, v_N]^T \\ \boldsymbol{\Phi} &= [\boldsymbol{\phi}_1, \ldots, \boldsymbol{\phi}_N]^T. \end{aligned} \tag{30}$$

Given that the battery (V, Q) data are collected at a fixed sample of Q points, $\boldsymbol{\Phi}$ in (29) is a constant matrix for all time. Therefore, the parameter $\boldsymbol{\theta}$ can be simply calculated as

$$\boldsymbol{\theta} = \mathbf{h}^T \mathbf{V} \tag{31}$$

where

$$\mathbf{h} = \boldsymbol{\Phi} \left(\boldsymbol{\Phi}^T \boldsymbol{\Phi}\right)^{-1} \tag{32}$$

is a constant matrix and can be computed offline.

The computational time of using the LP-SVR and the LSM for the $V-Q$ curve identification are compared in Table I. The four groups of data are sampled within the same range of charged capacity but with different sampling rate; therefore, the results of different sizes of data could also be compared. One can see that the computational time of the LSM takes far less than that of the LP-SVR and is insensitive to the dimension of sampled data.

TABLE I
COMPUTATIONAL TIME COMPARISON

# of Data Points	LP-SVR (sec.)	LSM (sec.)
20	0.4733	0.000011
50	4.201	0.000011
100	30.01	0.000011
200	211.5	0.000016

†The assessment summarized in Table I was performed on a laptop computer with a 32-bit Intel Core2 Duo CPU @ 2.53 GHz and 4.0 GB RAM

The parametric battery $V-Q$ curve model provides a more robust and computationally efficient way to obtain the IC curves from raw data measurement without sacrificing any estimation accuracy.

VI. CONCLUSION

This paper has reported the findings of exploiting the parametric SVR model for real-time battery system characterization and proposed a framework for lithium-ion battery SOH monitoring. To investigate the sensitivity of the parametric structure to battery voltage data variation, a parametric LP problem is formulated. The voltage variation is characterized through simulations using mechanistic battery aging model and verified using battery test data. The parametric LP is solved by Monte Carlo simulations. Because of the data characteristics, the SVs in the $V-Q$ curve model of $LiFePO_4$ battery do not change, even when the battery cells age or vary. A model parametrization based on the SV invariance is thereby established. The resulting linear parametric model can be directly implemented in onboard BMS for SOH monitoring.

REFERENCES

[1] S. M. Schoenung and W. V. Hassenzahl, "Long- versus Short-Term energy storage technologies analysis: A life-cycle cost study," Sandia Nat. Lab., Albuquerque, NM, USA, Tech. Rep. SAND2003-2783, Aug. 2003.

[2] B. Dunn, H. Kamath, and J.-M. Tarascon, "Electrical energy storage for the grid: A battery of choices," *Science*, vol. 334, no. 6058, pp. 928–935, Nov. 2011.

[3] M. Grünig, M. Witte, D. Marcellino, J. Selig, and H. van Essen, "An overview of electric vehicles on the market and in development," Tech. Rep., CE Delft, Delft, The Netherlands, Apr. 2011.

[4] P. Mock, S. A. Schmid, and H. E. Friedrich, "Market prospects of electric passenger vehicles," in *Electric and Hybrid Vehicles: Power Sources, Models, Sustainability, Infrastructure and the Market*, G. Pistoia, Ed. Amsterdam, The Netherlands: Elsevier, 2010.

[5] M. Armand and J. M. Tarascon, "Building better batteries," *Nature*, vol. 451, pp. 652–657, Feb. 2008.

[6] A. Khaligh and Z. Li, "Battery, ultracapacitor, fuel cell, hybrid energy storage systems for electric, hybrid electric, fuel cell, plug-in hybrid electric vehicles: State of the art," *IEEE Trans. Veh. Technol.*, vol. 59, no. 6, pp. 2806–2814, Jul. 2010.

[7] M. A. Roscher, J. Assfalg, and O. S. Bohlen, "Detection of utilizable capacity deterioration in battery systems," *IEEE Trans. Veh. Technol.*, vol. 60, no. 1, pp. 98–103, Jan. 2011.

[8] M. A. Roscher and D. U. Sauer, "Dynamic electric behavior and open-circuit-voltage modeling of $LiFePO_4$-based lithium ion secondary batteries," *J. Power Sources*, vol. 196, no. 1, pp. 331–336, Jan. 2011.

[9] J. Kim and B. H. Cho, "State-of-charge estimation and state-of-health prediction of a li-ion degraded battery based on an ekf combined with a per-unit system," *IEEE Trans. Veh. Technol.*, vol. 60, no. 9, pp. 4249–4260, Nov. 2011.

[10] A. Szumanowski and Y. Chang, "Battery management system based on battery nonlinear dynamics modeling," *IEEE Trans. Veh. Technol.*, vol. 57, no. 3, pp. 1425–1432, May 2008.

[11] Z. Chen, C. C. Mi, Y. Fu, J. Xu, and X. Gong, "Online battery state of health estimation based on genetic algorithm for electric and hybrid vehicle applications," *J. Power Sources*, vol. 240, pp. 184–192, Oct. 2013.

[12] C. Weng, Y. Cui, J. Sun, and H. Peng, "On-board state of health monitoring of lithium-ion batteries using incremental capacity analysis with support vector regression," *J. Power Sources*, vol. 235, pp. 36–44, Aug. 2013.

[13] M. Dubarry, V. Svoboda, R. Hwu, and B. Y. Liaw, "Incremental capacity analysis and close-to-equilibrium OCV measurements to quantify capacity fade in commercial rechargeable lithium batteries," *Electrochem. Solid St.*, vol. 9, no. 10, pp. A454–A457, 2006.

[14] J. Groot, "State-of-Health Estimation of Li-Ion Batteries: Cycle Life Test Methods," M.S thesis, Chalmers Univ. Technol., Gothenburg, Sweden, 2012.

[15] M. Dubarry and B. Y. Liaw, "Identify capacity fading mechanism in a commercial $LiFePO_4$ cell," *J. Power Sources*, vol. 194, no. 1, pp. 541–549, Oct. 2009.

[16] X. Feng *et al.*, "Using probability density function to evaluate the state of health of lithium-ion batteries," *J. Power Sources*, vol. 232, pp. 209–218, Jun. 2013.

[17] X. Han *et al.*, "A comparative study of commercial lithium ion battery cycle life in electrical vehicle: Aging mechanism identification," *J. Power Sources*, vol. 251, pp. 38–54, Apr. 2014.

[18] A. J. Smith and J. R. Dahn, "Delta differential capacity analysis," *J. Electrochem. Soc.*, vol. 159, no. 3, pp. A290–A293, 2012.

[19] I. Bloom *et al.*, "Differential voltage analyses of high-power, lithium-ion cells 1. technique and application," *J. Power Sources*, vol. 139, no. 1/2, pp. 295–303, Jan. 2005.

[20] K. Honkuraa, H. Honboa, Y. Koishikawab, and T. Horibab, "State analysis of lithium-ion batteries using discharge curves," *ECS Tran.*, vol. 13, no. 19, pp. 61–73, 2008.

[21] K. Honkuraa, K. Takahashia, and T. Horibab, "Capacity-fading prediction of lithium-ion batteries based on discharge curves analysis," *J. Power Sources*, vol. 196, no. 23, pp. 10141–10147, Dec. 2011.

[22] H. Drucker, C. J. C. Burges, L. Kaufman, A. Smola, and V. Vapnik, "Support vector regression machines," in *Proc. Adv. Neural Inf. Process. Syst.*, 1997, pp. 155–161.

[23] C. Cortes and V. Vapnik, "Support-vector networks," *Mach. Learn.*, vol. 20, no. 3, pp. 273–297, Sep. 1995.

[24] B. E. Boser, I. M. Guyon, and V. N. Vapnik, "A training algorithm for optimal margin classifiers," in *Proc. 5th Annu. ACM Workshop Comput. Learn. Theory*, 1992, pp. 144–152.

[25] A. J. Smola and B. Schölkopf, "A tutorial on support vector regression," *Stat. Comput.*, vol. 14, no. 3, pp. 199–222, Aug. 2004.

[26] Y.-J. Lee and O. L. Mangasarian, RSVM: Reduced Support Vector Machines, Data Mining Inst. Comp. Sci. Dept., Univ. Wisconsin, Madison, WI, USA, Tech. Rep. 00-07. [Online]. Available: ftp://ftp.cs.wisc.edu/pub/dmi/tech-reports/00-07.ps

[27] B. Schölkopf and A. J. Smola, *Learning with Kernels: Support Vector Machines, Regularization, Optimization, Beyond*, 1st ed. Cambridge, MA, USA: MIT Press, Dec. 2001.

[28] T. Hofmann, B. Schölkopf, and A. J. Smola, "Kernel methods in machine learning," *Ann. Statist.*, vol. 36, no. 4, pp. 1171–1220, Jul. 2008.

[29] N. Cristianini and J. Shawe-Taylor, *An Introduction to Support Vector Machines and Other Kernel-Based Learning Methods*, 1st ed. Cambridge, U.K.: Cambridge Univ. Press, Mar. 2000. [Online]. Available: http://www.cambridge.org/gb/knowledge/isbn/item1166741/?site_locale=en_GB

[30] V. N. Vapnik, *The Nature of Statistical Learning Theory*, 1st ed. New York, NY, USA: Springer-Verlag, 1995.

[31] V. Cherkassky and Y. Ma, "Practical selection of SVM parameters and noise estimation for SVM regression," *Neural Netw.*, vol. 17, no. 1, pp. 113–126, Jan. 2004.

[32] A. J. Smola, T. T. Frieß, and B. Schölkopf, "Semiparametric support vector and linear programming machines," Neural Computational Learning II, London, U.K., NeuroCOLT2 Tech. Rep. NC2-TR-1998-024, Aug. 1998, 27150.

[33] X. Hu, S. Li, and H. Peng, "A comparative study of equivalent circuit models for li-ion batteries," *J. Power Sources*, vol. 198, pp. 359–367, Jan. 2012.

[34] C. Weng, J. Sun, and H. Peng, "A unified open-circuit-voltage model of lithium-ion batteries for state-of-charge estimation and state-of-health monitoring," *J. Power Sources*, vol. 258, pp. 228–237, Jul. 2014.

[35] B. Y. Liaw and M. Dubarry, "A roadmap to understand battery performance in electric and hybrid vehicle operation," in *Electric and Hybrid Vehicles: Power Sources, Models, Sustainability, Infrastructure and the Market*, G. Pistoia, Ed. Amsterdam, The Netherlands: Elsevier, 2010.

[36] A. Smith, "A high precision study of li-ion batteries," Ph.D. dissertation, Dalhousie Univ., Halifax, NS, Canada, 2012.

[37] Z. Lu, J. Sun, and K. Butts, "Linear programming SVR-ARMA$_2k$ with application in engine system identification," *IEEE Trans. Autom. Sci. Eng.*, vol. 8, no. 4, pp. 846–854, Oct. 2011.

[38] Z. Lu, J. Sun, and K. Butts, "Linear programming support vector regression with wavelet kernel: A new approach to nonlinear dynamical system identification," *Math. Comput. Simulat.*, vol. 79, no. 7, pp. 2051–2063, Mar. 2009.

[39] G. Bloch, F. Lauer, G. Colin, and Y. Chamaillard, "Support vector regression from simulation data and few experimental samples," *Inf. Sci.*, vol. 178, no. 20, pp. 3813–3827, Oct. 2008.

[40] A. Gretton, A. Doucet, R. Herbrich, P. Rayner, and B. Schölkopf, "Support vector regression for black-box system identification," in *Proc. 11th IEEE Workshop Statist. Signal Process.*, Aug. 2001, pp. 341–344.

[41] A. Smola, B. Schölkopf, and G. Ratsch, "Linear programs for automatic accuracy control in regression," in *Proc. 9th Int. Conf. Artif. Neural Netw.*, Edinburgh, U.K., Sep. 1999, vol. 2, pp. 575–580.

[42] J. Bi, K. Bennett, M. Embrechts, C. Breneman, and M. Song, "Dimensionality reduction via sparse support vector machines," *J. Mach. Learn. Res.*, vol. 3, pp. 1229–1243, Mar. 2003.

[43] O. L. Mangasarian and D. R. Musicant, "Large scale kernel regression via linear programming," *Mach. Learn.*, vol. 46, no. 1–3, pp. 255–269, 2002.

[44] D. Bertsimas and J. N. Tsitsiklis, *Introduction to Linear Optimization*. Belmont, MA, USA: Athena Scientific, 1997.

[45] I. Adler and R. D. C. Monteiro, "A geometric view of parametric linear programming," *Algorithmica*, vol. 8, no. 1–6, pp. 161–176, Dec. 1992.

[46] M. Dubarry, C. Truchot, and B. Y. Liaw, "Synthesize battery degradation modes via a diagnostic and prognostic model," *J. Power Sources*, vol. 219, pp. 204–216, Dec. 2012.

[47] E. Prada, D. Di Domenico, Y. Creff, J. Bernard, V. Sauvant-Moynot, and F. Huet, "A simplified electrochemical and thermal aging model of $LiFePO_4$-graphite li-ion batteries: Power and capacity fade simulations," *J. Electrochem. Soc.*, vol. 160, no. 4, pp. A616–A628, 2013.

[48] P. Albertus, J. Couts, V. Srinivasan, and J. Newman, "A combined model for determining capacity usage and battery size for hybrid and plug-in hybrid electric vehicles," *J. Power Sources*, vol. 183, no. 2, pp. 771–782, Sep. 2008.

Caihao Weng received the B.S.E. and M.S.E. degrees from the University of Michigan, Ann Arbor, MI, USA, in 2010 and 2013. He is currently working toward the Ph.D. degree with the Department of Naval Architecture and Marine Engineering, University of Michigan.

His research interests include data-driven modeling, system identification, and mathematical optimization with applications to adaptive battery management systems.

Jing Sun (M'89–SM'00–F'04) received the B.S. and M.S. degrees from the University of Science and Technology of China, Hefei, China, in 1982 and 1984, respectively, and the Ph.D. degree from the University of Southern California, Los Angeles, CA, USA, in 1989.

From 1989 to 1993, she was an Assistant Professor with the Department of Electrical and Computer Engineering, Wayne State University, Detroit, MI, USA. In 1993, she joined the Powertrain Control Systems Department, Ford Research Laboratory. After spending almost ten years in industry, she came back to academia and joined the faculty of the College of Engineering, University of Michigan, Ann Arbor, MI, USA, in 2003, where she is currently a Professor with the Department of Naval Architecture and Marine Engineering and the Department of Electrical Engineering and Computer Science. She is a holder of 37 U.S. patents and is a coauthor of the textbook *Robust Adaptive Control* (Courier Dover, 2012). Her research interests include system and control theory and its applications to marine and automotive propulsion systems.

Dr. Sun coreceived the IEEE Control System Technology Award in 2003.

Huei Peng received the Ph.D. degree in mechanical engineering from the University of California, Berkeley, CA, USA, in 1992.

He is currently a Professor with the Department of Mechanical Engineering, University of Michigan, Ann Arbor, MI, USA. Over the last ten years, he has been involved in the design of several military and civilian concept vehicles, including Future Tactical Truck Systems, Family of Medium Tactical Vehicles, Eaton/Fedex, and Super-HUMMWV, for both electric and hydraulic hybrid concepts. He is currently the U.S. Director of the Department of Energy (DOE) sponsored Clean Energy Research Center—Clean Vehicle Consortium, which supports more than 30 research projects related to the development of clean vehicles in the U.S. and China. He also leads an educational project funded by DOE to develop ten undergraduate and graduate courses, including three laboratory courses focusing on transportation electrification. He serves as the Associate Director of the University of Michigan Mobility Transformation Center: a center that studies connected and autonomous vehicle technologies and promotes their deployment. He has served as the Principal Investigator (PI) or Co-PI of more than 50 research projects, with a total funding of more than $30 million. He has more than 240 technical publications, including 105 in referred journals and transactions and four books. His h-index is 50 according to the Google scholar analysis, and the total number of citations to his work is more than 9400. His main research interests include adaptive control and optimal control, with emphasis on their applications to vehicular and transportation systems. His current research interests include design and control of electrified vehicles and connected/automated vehicles.

Dr. Peng received the National Science Foundation Career Award in 1998. He is a ChangJiang Scholar at the Tsinghua University of China. He is a Fellow of the Society of Automotive Engineers and the American Society of Mechanical Engineers.